Contents lists available at ScienceDirect

Scientific African

journal homepage: www.elsevier.com/locate/sciaf

Synthesis, molecular docking studies and ADME prediction of some new triazoles as potential antimalarial agents

Francis Klenam Kekessie [a], Cedric Dzidzor Kodjo Amengor [b,*], Abena Brobbey [a],
John Nii Addotey [a], Cynthia Amaning Danquah [c], Paul Peprah [b],
Benjamin Kingsley Harley [d], Inemesit Okon Ben [e], Felix Kwame Zoiku [f],
Lawrence Sheringham Borquaye [g,h], Edward Ntim Gasu [g,h], Ebenezer Ofori-Attah [i],
Michael Tetteh [a]

[a] Department of Pharmaceutical Chemistry, Faculty of Pharmacy and Pharmaceutical Sciences, Kwame Nkrumah University of Science and Technology, Kumasi, Ghana
[b] Department of Pharmaceutical Chemistry, School of Pharmacy, University of Health and Allied Sciences, Ho, Ghana
[c] Department of Pharmacology, Faculty of Pharmacy and Pharmaceutical Sciences, Kwame Nkrumah University of Science and Technology, Kumasi, Ghana
[d] Department of Pharmacognosy, School of Pharmacy, University of Health and Allied Sciences, Ho, Ghana
[e] Department of Pharmacology, School of Pharmacy, University of Health and Allied Sciences, Ho, Ghana
[f] Department of Epidemiology, Noguchi Memorial Institute for Medical Research, Legon, Accra, Ghana
[g] Department of Chemistry, Kwame Nkrumah University of Science and Technology, Kumasi, Ghana
[h] Central Laboratory Complex, Kwame Nkrumah University of Science and Technology, Kumasi, Ghana
[i] Department of Clinical Pathology, Noguchi Memorial Institute for Medical Research, Legon, Accra, Ghana

ARTICLE INFO

ABSTRACT

The challenges concerning the control of malaria remain due to the continuous emergence of drug resistant strains. Over the years, the use, misuse, and abuse of antimalarials have created a conducive environment for the development of resistant Plasmodium falciparum strains. We herein report on the synthesis, characterization and antimalarial activity of a library of seven novel 1,2,3-triazoles as part of the drug discovery campaign against drug-resistant Plasmodium falciparum. The interactions of the triazoles with plasmepsin II, plasmepsin IV, falcipain-2 and the heme detoxifying protein-all key proteins of Plasmodium falciparum degradosequesterome (Dsq) were also investigated by molecular docking. The compounds 3a-d, 4–6 were synthesized by CuAAC click reaction in good to excellent yields of 73–98% and characterized by melting point, UVvisible, infrared and nuclear magnetic resonance (^{1}H and ^{13}C) and MS techniques. Compounds 3a-d displayed high in vitro potency (IC_{50}s: 0.62–22.11 ug/ml) against the chloroquine-resistant Dd2 lab strain of Plasmodium falciparum and low toxicity (SI > 1 except compound 4) to human erythrocytes. Computational studies indicated that the compounds 3a-3d had an absorption of 76–91%, and they were category III acute oral toxins (LD_{50} from 500 to 5000 mg/kg). The molecular docking study suggests that compounds 3a-d interacted with plasmepsin IV and the heme detoxifying protein with high affinity and a moderate affinity for falcipain-2.

© 2021 Published by Elsevier B.V. on behalf of African Institute of Mathematical Sciences / Next Einstein Initiative.
This is an open access article under the CC BY-NC-ND license (http://creativecommons.org/licenses/by-nc-nd/4.0/)
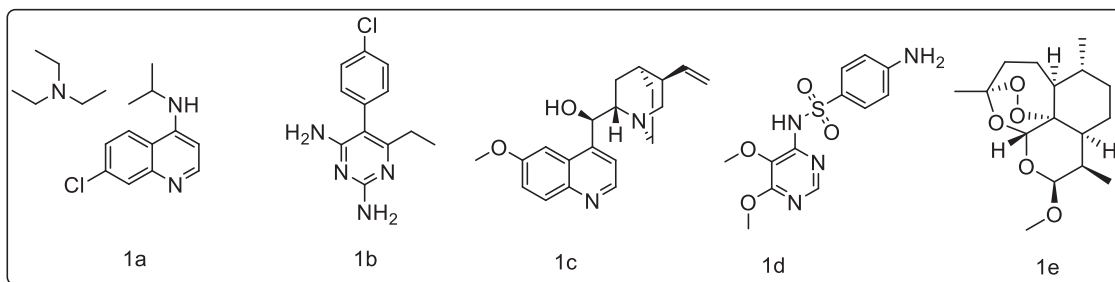
Fig 1. Some antimalarials which have reported issues of pathogen resistance.

Introduction

The discovery of drugs for infectious diseases remains part of the priority list in the field of medicinal chemistry due to the increasing mortality and morbidity of infections [1, 2]. The global statistics on infectious diseases are disturbing, with over 17 million deaths recorded annually, making WHO declare the situation as a global crisis since 2019 [3]. Among these infectious diseases, parasitic diseases are the largest contributors to the mortality rate recorded. The contributing factors to the slow pace of defeating infections include the development of resistance mechanisms (biofilm inhibition, efflux pumps, and quorum sensing) against existing chemotherapy [4]. Parasitic infections such as malaria-caused by the protozoan Plasmodium falciparum-remain prevalent in many tropical countries [5]. Malaria causes an annual estimated 627,000 deaths world-wide and this has been attributed mainly to the action of drug-resistant parasites [6] and the situation is growing worse despite efforts by stakeholders in the regulatory and pharmaceutical industry to manage the situation [7]. Over the years, several antimalarial drugs (either natural or synthetic) have become less effective due to increasing resistance by the Plasmodium parasites [8]. These panels of drugs include chloroquine (1a), pyrimethamine (1b), quinine (1c), artemisinin derivatives (eg. Artemether (1d) and sulphadoxine (1e) (Fig. 1).

It is also necessary to understand the life cycle of the parasite, which would lead to the discovery of better drug targets. Various mechanisms of action have been proposed for the antiplasmodial action of some antimalarial drugs. These include inhibition of key enzymes involved in folate and nucleotide biosynthesis, such as dihydropteroate synthase (DHPS), dihydrofolate reductase (DHFR) and dihydroorotate dehydrogenase (DHODH). Pyrimethamine and sulfadoxine are known to target DHFR and DHPS respectively [9]. hemoglobin (Hb) is a major need of the parasite in the intra-erythrocytic stage. In P. falciparum malaria, Hb degradation produces protein digest products and free-heme, the latter of which is converted to hemozoin (Hz) [10]. The presence of free-heme in the parasite's food vacuole (FV) is lethal, hence heme detoxification via Hz formation. Chloroquine (CQ) and artemisinin have both been shown to act by targeting the heme polymerization step. Additionally, CQ inhibits Hb degradation [11]. Thus, hemoglobin degradation and heme polymerization are also attractive drug targets [12]. The P. falciparum degradosequesterome (Dsq) is a 200 KDa protein complex responsible for hemoglobin degradation and conversion of free heme to hemozoin, making the complex an important drug target. Essentially, this complex is made up of aspartic proteases-plasmepsins (Plms) II and IV-, cysteine proteases-Falcipain2/2 '(PfFP2/2′)-and the heme detoxifying protein (PfHDP). Plms II cleaves native hemoglobin at a specific site (33–34). Interestingly, Plms II is able to further cleave denatured globin into even smaller peptides and hence supply valuable amino acids needed for parasite survival. Plms IV plays a similar role to Plms II and both are localized in the food vacuole of the parasite [13, 14, 15]. Falcipains are also localized in the food vacuole of the parasite, and, together with the plasmepsins and other enzymes, are involved in hemoglobin degradation. Falcipains 2 hydrolyze hemoglobin at multiple sites. Falcipains have also been suggested to be involved in the cleavage of plasmepsins into their more active proteinase forms. In particular, falcipain 2 hydrolyses 2 important proteins that make up the cytoskeleton of erythrocytes – protein 4.1 and ankyrin. Lastly, PfHDP is an extremely potent enzyme that is responsible for the conversion of toxic heme to the more tolerable hemozoin in the parasite. The gene that encodes HDP is functionally conserved across all species in the Plasmodium genus [16]. Together, these enzymes are important targets whose inhibition will lead to parasite death, and hence attractive targets for the development of malaria therapeutic agents. In silico experiments on the Dsq of P. falciparum are limited due to the unavailability of the solved crystal structure of the PfHDP [17]. Though prone to some predictive errors in the absence of closely-related experimental templates, homology modeling and molecular dynamics have contributed significantly to drug discovery in such cases. Understanding the interactions between potential antiplasmodial lead compounds and the proteins that make up the Dsq could potentially provide insights into plausible modes of action and suggest possible routes for lead optimization. hemoglobin (Hb) is a major need of the parasite in the intra-erythrocytic stage and in P. falciparum malaria, Hb degradation

---

* Correspondence author.
  E-mail address: camengor@uhas.edu.gh (C.D.K. Amengor).
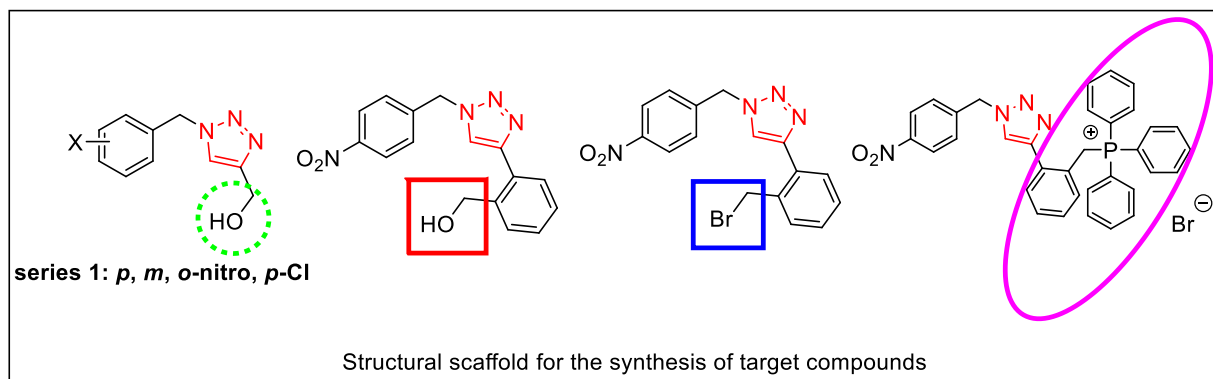
Fig 2. Structural scaffolds for synthesis of the target compounds.

produces free-heme, which is converted to hemozoin (Hz). The presence of free-heme in the parasite's food vacuole (FV) is lethal, hence prevention of heme degradation in malaria chemotherapy is one of the main focus.

However, the continuous quest for novel effective drugs by medicinal chemists has led to the development of relatively simple and systematic processes for the generation of a new library of compounds for biological screening against Plasmodium falciparum [18].

This has made medicinal chemists particularly interested in synthetic routes that provide uncomplicated access to large compound databases for selection in malaria chemotherapy [19]. The employment of these rapid synthetic pathways allows the production of potential biologically useful compounds in a short period of time, thus hastening the lead optimization and general drug discovery process. The salient characteristics of an ideal synthetic strategy, apart from its rapidity, include selectivity, versatility, and productivity. One synthetic process that fulfills these requirements is the 1, 3-dipolar cycloaddition reaction, which is also referred to as Huisgen cycloaddition [20]. In recent times, cycloaddition reactions have been templates for the construction of biologically active compounds with five-membered heterocyclic ring (s) [21]. In the chemical topography of these reactions, copper or ruthenium have been the best catalysts for the coupling of an azide and an alkyne to yield the 1,2,3-triazole ring [22]. Although Huisgen's postulate was discovered in the 20th century, its longstanding advantages include products of versatile biological activity, metabolic stability, and resistance to acid and base hydrolysis. This has given huge momentum to current trends in drug discovery. Among the 1,2,3-triazoles, the 1,4-disubstituted analogues are most ubiquitously synthesised via the 1,3-dipolar cycloaddition. However, the Huisgen 1,3-dipolar cycloaddition has received considerable interest due to the introduction of Cu (I) catalysts in the copper catalysed azide alkyne [3 + 2] cycloaddition by Sharpless, which enhances the reaction rate, regioselectivity and chemoselectivity. This concept makes these Cu (I) reactions successful in terms of quantitative yields, robustness, orthogonal and bio-molecular conjugation. These features introduced the concept of click reaction (linking two pharmacophores), which is defined as a set of reactions which are wide in scope, easy to perform, high yielding with little or no work-up and purification, and have favourable thermodynamics and kinetics [23]. Clicking means joining two pharmacophores together using 1,2,3-triazole as the linker. The importance of studying the chemistry of 1,2,3 triazoles remains incessant due to their use for the hybridization of pharmacophores.

Nevertheless, in recent times, there has been considerable interest in tethering triazoles to positively charged compounds such as quartenary phosphonium salts due to their feasibility of synthesis and excellent established wide spectrum of biological activities [24]. With this caveat in mind, in the current study, quartenary phosphonium salt was the final target after hybridization using the 1, 2, 3 triazoles as a linker in one of series 1 as a preliminary data for building more libraries. Furthermore, a comprehensive overview of the use of these heterocycles as linkers has been reported by [25].

This current research is aimed at employing substituted benzyl bromides and an aliphatic/aromatic alkyne for the synthesis of new 1,2,3-triazole derivatives and a tethered quartenary phosphonium salt as part of click reactions application in drug discovery. This concept is represented by the structural scaffold for the synthesis of the target compounds (series 1–4) (Fig. 2).

Hence this present study reports the synthesis of a library of 1,2,3-triazoles followed by in silico prediction and in vitro antimalarial evaluation.

Experimental

Chemistry

General. All solvents and reagents for the syntheses of target compounds were obtained from commercially available sources including, Sigma-Aldrich (United Kingdom), Fisher Scientific (United Kindgom) and Fluorochem (United Kingdom). Thin-layer-chromatography (TLC) analysis was performed on silica gel plates (E. Merck silica gel 60 F254 plates) and visualized with ultraviolet (UV) lamp at 254 nm and 365 nm. The compounds were purified by gravity column chromatography

with silica gel as a stationary phase (Merck 60, 230−400 mesh). Compounds were run neat to obtain the infrared (IR) spectra on a Bruker FTIR spectrophotometer (Germany) mounted with platinum ATR. ^{1}H, ^{13}C nuclear magnetic resonance (NMR) and DEPT-135 analysis were performed on a Bruker Ascend FT NMR 500 MHz spectrometer (NM 103,508–10, Germany) using TMS as the internal standard. High resolution mass spectra (MS) was obtained from a 6420 Triple Quad with an electrospray ionization source from Agilent Technologies. The purity of all tested compounds was determined by analytical RP-HPLC in tandem with MS using Agilent 1290 infinity series (and a Mightysil C18 column (150 mm x 4.6 mm, 15 μm) using an isocratic elution system (distilled water: acetonitrile, 7:3% v/v) at a flow rate of 1 ml/min equipped with a photodiode array (PDA) detection wavelength at 270 nm. Mass spectra were registered in the ESI+ mode. Uncorrected melting points were determined by open capillary method using a Stuart SMP30 melting point apparatus. All the compounds tested for their biological activity were >90% pure, confirmed with MassHunter Software for HPLC-MS. Scanned spectra for all compounds are shown in Figure SM1-SM35. Grid search box dimensions used for the respective protein targets were as follows;

PfHDP (center; x: 45.33, y: 23.46, z: 44.2767; size: x: 26.2067, y: 34.0, z: 32.7075), PfFP2 (center; x: 19.53, y: −39.15, z: 8.16; size: x: 20.30, y: 16.30, z: 15.61), PlmsII (center; x: 0.28, y: −12.51, z: −47.98; size: x: 20.50, y: 23.64, z: 24.74), and PlmsIV (center; x: −28.3863, y: 37.77, z: 40.48; size: x: 20.50, y: 23.64, z: 24.74). PlmsII and IV were used in method validation of molecular docking by re-docking native ligands to the binding pockets of the respective receptors. The determinants of ligand binding were explored by molecular docking in UCSF Chimera extended to include AutoDock Vina, whereas protein-ligand (PL) interactions were visualized in Discovery Studio (DS, version 2020, Accelrys Software Inc.).

General procedure for the synthesis of the azides (2a-2d) [26]

Schemes for the azides represented in figure SM36- Figure SM39

The substituted benzyl bromides (1equiv, 5 mmol) and sodium azide (NaN$_3$) (3.0 equiv, 15 mmol) were transferred into a round bottom reaction flask (50 mL) equipped with magnetic stir bar. This was followed by the addition of water: acetone (3:1, 10 mL). The mixture was stirred at 26 °C for 12 h. The reaction was monitored by TLC. After the reaction was complete, it was quenched by addition of water (10 mL). This was followed by the addition of ethyl acetate (20 mL) before the mixture was transferred into a separatory funnel and worked up with ethyl acetate (3 × 50 mL). The combined organic portions were washed with brine (50 mL). The organic phase was dried over anhydrous sodium sulfate (Na$_2$SO$_4$) and the filtrate concentrated under reduced pressure to afford pale to deep yellow oils.

General procedure for the synthesis of the 1,4 disubstituted 5H, 1,2,3-triazoles (3a-d,4) [27]

Distilled water (10 mL) was added to the substituted benzyl azides (1 equiv.) in a 50 mL round bottom flask equipped with magnetic stirrer and the mixture stirred for 10 min. The alkyne (propargyl alcohol/2-ethynyl benzyl alcohol) (1.2 equiv.), CuSO$_4$•5H$_2$O (0.05 equiv.) and L-sodium ascorbate (1 equiv.) were added and the reaction monitored by TLC. After completion of the reaction, the mixture was diluted with 20 mL each of water and diethyl ether. The resulting mixture was transferred into a separatory funnel and the organic phase (diethyl ether portion) separated. The aqueous phase was extracted with diethyl ether (2 × 50 mL). The combined organic phase was washed with brine (50 mL). The resulting organic phase was dried with anhydrous sodium sulfate and the filtrate concentrated under reduced pressure to obtain a pale yellow solid. The crude product was directly chromatographed on silica column using ethyl acetate/petroleum ether (9:1%v/v) as the eluent to afford the product as a solid which was used for the next step (bromination).

General procedure for the bromination of the triazoles (5) [28]

Into a 50 mL round bottom flask, equipped with a magnetic stirrer, under nitrogen atmosphere, the triazole in step 2 was dissolved in anhydrous CH$_2$Cl$_2$ (30 mL). The mixture was cooled to 0 °C in an ice bath and phosphorus tribromide added dropwise. The mixture was stirred for 20 min and allowed to warm to room temperature. After 1.5 h, a white cloudy reaction mixture was observed and the reaction was quenched by diluting with distilled water (100 mL) after transferring into an Erlenmeyer flask (250 mL), followed by dropwise addition of saturated Na$_2$CO$_3$ solution until effervescence ceased. The resulting solution was transferred into a separatory funnel and extracted with CH$_2$Cl$_2$ (3 × 50 mL). The combined organic phase was washed with brine (100 mL). The resulting organic portion was dried with anhydrous Na$_2$SO$_4$ and the filtrate was concentrated under reduced pressure to obtain a pale yellow solid. The crude product which was purified by column chromatography to afford a white solid which was used in the last step (phosphonium salt synthesis).

General procedure for the synthesis of the phosphonium salt (6) [29]

Into a round bottom flask equipped with magnetic stir bar under balloon filled nitrogen with toluene (20 mL) as a solvent followed by triphenylphosphine (1.10 equiv) and allowed to stir for 10 min to obtain a clear solution. This was followed by the addition of the brominated triazole compound (1 equiv.). The reaction medium was heated under reflux at 120 °C for 16 hrs until the appearance of solid precipitate. The reaction mixture was allowed to cool to room temperature and filtered under pressure to afford a white solid.

Spectral data

Propargyl alcohol derivatives

(1-(4-nitrobenzyl)−1H-1,2,3-triazole-4-yl)methanol (3a). R$_f$: 0.40 (EtOAc: Pet. ether [60:40–95:5]); Yield: 95%, mpt 130–134 °C; IR (neat) (cm^{-1}): 3260 (CH$_2$OH), 3308 (alkyne C–H stretch), 1414 (*C = N*). ^{1}H NMR (500 MHz, DMSO) δ 7.85–7.80 (2 H, m, C(3)H$_{Ar}$, C(5) H$_{Ar}$); 7.61 (1 H, s, C(1″)H$_{triazole}$); 7.77–7.74 (2 H, m, C(2)H$_{Ar}$, C(6)H$_{Ar}$); 5.27 (2H, s, C(1′)H$_2$); 5.02–4.96 (1 H, t, *J* = 5.00 Hz, CH$_2$OH); 4.09–4.05 (2 H, d, C(3″), *J* = 5.00 Hz CH$_2$OH). ^{13}C NMR (500 MHz, DMSO) δ 149.0, 148.0, 147.0, 145.0, 143.0, 142.0, 130.0, 125.0, 57.0 (1′C), 52.0, (3″C), HRMS (ESI): *m/z* calculated for [*M + H*]$^+$ C$_{10}$H$_{10}$N$_4$O$_3$, 234.21, found 235.10.

(1-(3-nitrobenzyl)−1H-1,2,3-triazole-4-yl)methanol (3b). R$_f$: 0.37 (EtOAc: Pet ether [60:40–95:5]); Yield: 92%; mpt 86–89 °C; IR (neat) (cm^{-1}): 3284 (CH$_2$OH), 3151 (*C = C*–H), 1421 (*C = N*); ^{1}H NMR (500 MHz, DMSO) δ 8.31 (1H, m, C(4) H$_{Ar}$); 8.09 (1 H, s, C(1″)H$_{triazole}$); 7.78 (1 H, m, C(5)H$_{Ar}$); 7.70 (1 H, m, C(6)H$_{Ar}$); 5.77 (2 H, s, (C1′)H$_2$); 5.22 (1 H, t, *J* = 5.60 Hz, CH$_2$OH); 4.53 (2 H, d, *J* = 3.80 Hz, (C3″), CH$_2$OH). ^{13}C NMR (500 MHz, DMSO) δ 140.0, 138.0, 135.0, 133.0, 130.0, 125.0, 124.0, 125.0 (Ar), 56.0 (1′C), 52.0, (3″C), MS (ESI): *m/z* calculated for [*M + H*]$^+$ C$_{10}$H$_{10}$N$_4$O$_3$, 234.21, found 235.20

(1-(2-nitrobenzyl)−1H-1,2,3-triazole-4-yl)methanol (3c). R$_f$: 0.35 (Ethyl acetate: petroleum ether [60:40–95:5]); Yield: 73% mp 126–130 °C; IR (neat) (cm^{-1}): 3230 (CH$_2$OH), 3110 (*C = C*–H), 1410(*C = N*). ^{1}H NMR (500 MHz, DMSO) δ$_H$ 8.15–8.13 (1H, m, C(3)H$_{Ar}$); 8.02 (1 H, s, C(1″)H$_{triazole}$); 7.76–7.72 (1H, m, C(4)H$_{Ar}$), 7.63–7.62 (1H, m, C(5)H$_{Ar}$), 7.05–7.03 (1H, m, C(6)H$_{Ar}$), 5.94 (2H, s, C(1′)H$_2$), 5.27 (1H, m, CH$_2$OH), 4.54 (2 H, m, (C3″), CH$_2$OH). ^{13}C NMR (500 MHz, DMSO) δ$_c$ 140.0, 137.0, 135.0, 132.0, 131.0, 129.0, 125.0, 122.0, 56.0 (1′C), 51.0, (3″C); MS (ESI): *m/z* calculated for [*M + H*]$^+$ C$_{10}$H$_{10}$N$_4$O$_3$, 234.21, found 235.20.

(1-(4-chlorobenzyl)−1H-1,2,3-triazole-4-yl)methanol (3d). R$_f$: 0.42 (EtOAc: Pet ether [60:40–95:5]). Yield: 98%; mpt 84–88 °C; IR (neat) (cm^{-1}): 3284 (CH$_2$OH), 3151 (alkyne C–H stretch), 1420 (*C = N*). ^{1}H NMR (500 MHz, DMSO–d$_6$) δ 8.04 (1H, s, H$_{triazole}$); 7.47 - 7.44 (2H, m, C(3), C(5) H$_{Ar}$); 7.35–7.32 (2H, d, *J* = 8.4 Hz, C(2), C(6) H$_{Ar}$); 5.59 (2H, s, C(1′)H$_2$), 5.19 (1H, t, *J* = 5.7 Hz, CH$_2$OH), 4.52 (2H, d, *J* = 3.7 Hz, CH$_2$OH). ^{13}C NMR (500 MHz, DMSO–d$_6$) δ150.0, 134.0, 132.0, 130.0, 129.0, 121.0, 56.0 (1′C), 52.0, (3″C), MS (ESI): *m/z* calculated for [*M + H*]$^+$ C$_{10}$H$_{10}$N$_3$O^{35}Cl, 223.6600, found 224.2000; calculated C$_{10}$H$_{15}$N$_3$O^{37}Cl, 225.60, found, 226.20.

Synthesis of 2-ethynylbenzyl alcohol derivative

2-(1-(4-nitrobenzyl)−1H-1,2,3-triazol-4-yl) phenylmethanol (4). R$_f$: 0.52 (EtOAc: Pet ether [60:40–95:5]). Yield: 81% mpt: 132–135 °C; IR (neat) (cm^{-1}): 3260 (CH$_2$OH), 3083 (*C = C*–H), 1410(*C = N*). ^{1}H NMR (500 MHz, DMSO–d$_6$) δ 8.58 (1 H, s, C(1″)H$_{triazole}$); 8.27 (2 H, d, *J* = 6.90 Hz, C(3)H$_{Ar}$, C(5)H$_{Ar}$), 7.78 (1H, d, *J* = 6.90 Hz, C(2‴)H$_{Ar}$), 7.48 (1H, m, C(5‴)H$_{Ar}$), 7.46 (1H, m, C(4‴) H$_{Ar}$), 7.40 (1H, m, C(3‴)H$_{Ar}$), 7.37 (2H, m, C(2)H$_{Ar}$, C(6)H$_{Ar}$), 5.90 - 5.88 (2 H, m, C(1′)H$_2$), 5.75 (1H, t, *J* = 5.5 Hz, CH$_2$OH), 4.62 (1H, t, *J* = 5.6 Hz, C(3″)CH$_2$OH); ^{13}C NMR (500 MHz, DMSO–d$_6$) δ$_c$ 150.0, 148.0, 146.0, 145.0, 140.0, 132.0, 130.0, 129.0, 128.0, 127.0, 126.0, 124.0 (Ar), 62 (1′), 54 (7″C);MS (ESI): *m/z* calculated for [*M + H*]$^+$ C$_{10}$H$_{10}$N$_4$O$_3$, 310.31, found 311.20.

4-(2-bromomethyl)phenyl)−1-(4-nitrobenzyl)−1H-1,2,3-triazole (5). R$_f$: 0.62 (EtOAc: Pet ether [60:40–95:5]). Yield; 83%. mpt: 140–145 °C; IR (neat) (cm^{-1}): 1607 (*C = C*–H), 1412 (*C = N*), 670 (C-Br). ^{1}H NMR (500 MHz, DMSO–d$_6$) δ 8.12 (1 H, s, C(1″)H$_{triazole}$), 8.278 (2 H, d, *J* = 10.0 Hz, C(3)H$_{Ar}$, C(5)H$_{Ar}$), 7.61 (1H, m, C(2‴)H$_{Ar}$), 7.58 (1H, m, C(5‴)H$_{Ar}$), 7.47 (1H, m, C(4‴) H$_{Ar}$), 7.45 (1H, m, C(3‴)H$_{Ar}$), 7.42 (2H, m, C(2)H$_{Ar}$, C(6)H$_{Ar}$)H$_{Ar}$), 5.91 (2 H, m, C(1′)H$_2$), 5.75 (2H, s, CH$_2$Br); ^{13}C NMR (500 MHz, DMSO–d$_6$) δ 149.0, 147.0, 145.0, 140.0, 130.0, 128.0, 125.0, 132.0, 130.0, 129.0, 128.0, 127.0, (Ar), 62 (1′C), 52 (7″C). MS (ESI): *m/z* calculated for [*M + H*]$^+$ C$_{16}$H$_{14}$N$_4$O$_3$^{79}Br, 373.2100, found 373.2000, calculated for [*M + H*]$^+$ C$_{16}$H$_{14}$N$_4$O$_3$^{79}Br, 375.20, found C$_{16}$H$_{14}$N$_4$O$_3$^{81}Br, 375.21.

Synthesis of the tethered phosphonium salt

2-(1-(4-nitrobenzyl)−1H-1,2,3-triazol-4-yl)benzyl)triphenylphosphonium bromide (6). Yield; 92%; mp 240–245 °C; IR (neat) (cm^{-1}): 3284 (CH$_2$OH), 3151 (*C = C*–H), 1154 (C–N); ^{1}H NMR (500 MHz, DMSO–d$_6$,) δ$_H$ 8.29–8.26 (2H, m, C(3), C(5)H$_{Ar}$), 8.18 (1H, s, C(1′)H$_{triazole}$), 7.59 (1H, m, C(2‴)H$_{Ar}$),7.53 (1H, m, C(5‴)H$_{Ar}$), 7.59 (1H, m, C(4‴)H$_{Ar}$), 7.48 (1H, m, C(3‴)H$_{Ar}$), 7.64–7.63 (15H, m, H$_{ArP}$), 7.46–7.44 (2H, m, C(2), C(6)H$_{Ar}$), 5.76–5.73 (2H, d, *J* = 20.0 Hz, CH$_2$P), 5.68 (2H, s, C(2^1)H$_2$). ^{1}H NMR (500 MHz, DMSO–d$_6$,); δ$_c$ 147.0, 146.9, 143.1, 135.5, 134.1, 132.7, 131.3, 131.2, 132.7, 132.6, 130.5, 130.4, 130.3, 129.8, 129.5, 129.3, 129.1, 128.6, 128.5, 125.4, 124.3, 118.1, 117.1 (Ar), 52.4 1′(C), 27.3 (CH$_2$P); HRMS (ESI) *m/z* calculated for [M-Br]$^+$ C$_{34}$H$_{28}$N$_4$O$_2$P$^+$, 555.59, found 555.41.

Biological activity

Antiplasmodial activity

Cultivation, preparation of P. falciparum cultures for assay and plating of test compounds

The Plasmodium falciparum laboratory strain Dd2 was cultivated and prepared for assay and plating of the compounds according to method described by [30].

Fluorescence SYBR Green assay (in vitro antimalarial interaction assay)

The SYBR Green I-based fluorescence assay was employed according to [31] to investigate the in vitro antimalarial interaction between the seven (7) synthesised compounds with chloroquine and artesunate as the standard antimalarials (positive controls).

Absorbance measurement, visual inspection and statistical analysis

The inhibition percentage of each extract was determined by the equation:

$$Percent\ of\ growth\ inhibition = 1 + \left[\frac{Awell - Aneg}{Apos - Aneg} \right] x100$$

Where A_{neg} is the optical density of the negative control at 650 nm and Apos is the optical density of the positive control at 650 nm. Data were analyzed using the Genedata Screener program, Condoseo module (Genedata AG, Switzerland). Each compound was tested in triplicate and the concentration that inhibit asexual Plasmodium falciparum Dd2 lab strain by 50% (IC_{50}) were estimated from dose response curves by non-linear regression analysis using Graph pad Prism software (version 7.0 software San Diego, CA, USA).

Human erythroyctes in vitro cytotoxicity

The in vitro cytotoxic activity of each synthesized compounds was evaluated against K562 (human erythrocytes) using MTT colorimetric assay according to the previously published protocol [32]. Cell viability was calculated from the analysis.

$$Calculate\%\ cell\ viability = \left[\frac{Abs\ of\ treated\ well - Abs\ of\ color\ control}{Abs\ of\ untreated - Abs\ of\ blank} \right]$$

The concentrations at which 50% cytotoxic effect occurred (CC_{50} values) were then determined by plotting concentration of the compounds on the x-axis and percentage of cell viability on the y-axis with dose response curves (Using Microsoft Excel 2016 software). The CC50 values were compared with positive controls chloroquine and artesunate.

Computational methods

ADME prediction and toxicity

In silico pharmacokinetic and toxicity analyses of the compounds were carried out with ADMETlab and admetSAR, free online software for analysing ADMET properties of compounds. The physicochemical parameters of the compounds that were analysed include their molecular weights, number of hydrogen bond acceptors (HBA) and donors (HBD), topological polar surface areas (TPSA) and partition coefficients (cLogP). The absorption of the compounds were determined as follows: Percentage (%) Abs = 109 – (0.345 × TPSA) [33]. Parameters investigated to predict the toxicity of the compounds were hepatotoxicity, carcinogenicity, acute toxicity dose levels and Ames mutagenicity.

Molecular docking

Protein-target affinity screening

Vacuolar protein targets were selected. These were obtained from the protein databank (PDB) for Plms II, IV using the access codes 1LF3 and 1LS5 respectively. Falcipain2 co-crystalized with its (E) chalcone inhibitor (PDB ID: 6SSZ) [34] was used whereas the protein structural file of the heme detoxifying protein (HDP.pdb) was obtained from the report of Gupta and co-workers. Ligand structures and molecular docking were carried out using standard methods and tools described in the work of Borquaye and co-workers [35]. AutoDock Vina, extended in UCSF Chimera was used for ligand docking against target proteins. Protein-ligand interactions were visualized in Discovery Studio (DS, version 2020, Accelrys Software Inc.). Protein-ligand interactions were visualized in Discovery Studio (DS, version 2020, Accelrys Software Inc.). To validate docking protocols used in the study, the co-crystallized ligand bound to each protein obtained from the PDB was re-docked into the binding pockets of each protein. The docking protocol was evaluated to ensure that the re-docked output was similar to the crystal poses of their bound conformations extracted from the PDB. The root mean square deviations (RMSD) of the re-docked ligands were obtained using Pymol. For all docking experiments, 9 poses were obtained and evaluated. Each docking experiment was repeated in 5 technical runs to ensure reproducibility [36]. Validation of the docking protocols was done by re-docking.

Results and discussion

Chemistry

All tested compounds were synthesised with yields ranging from 73- 98%. This research includes the design and synthesis of new analogues of 1,4-disubstuted 1,2,3- compounds with different substituents and a tethered phosphonium salt. The target compounds (3a-d, 4–6) were synthesised according to the scheme presented in Fig. 3.
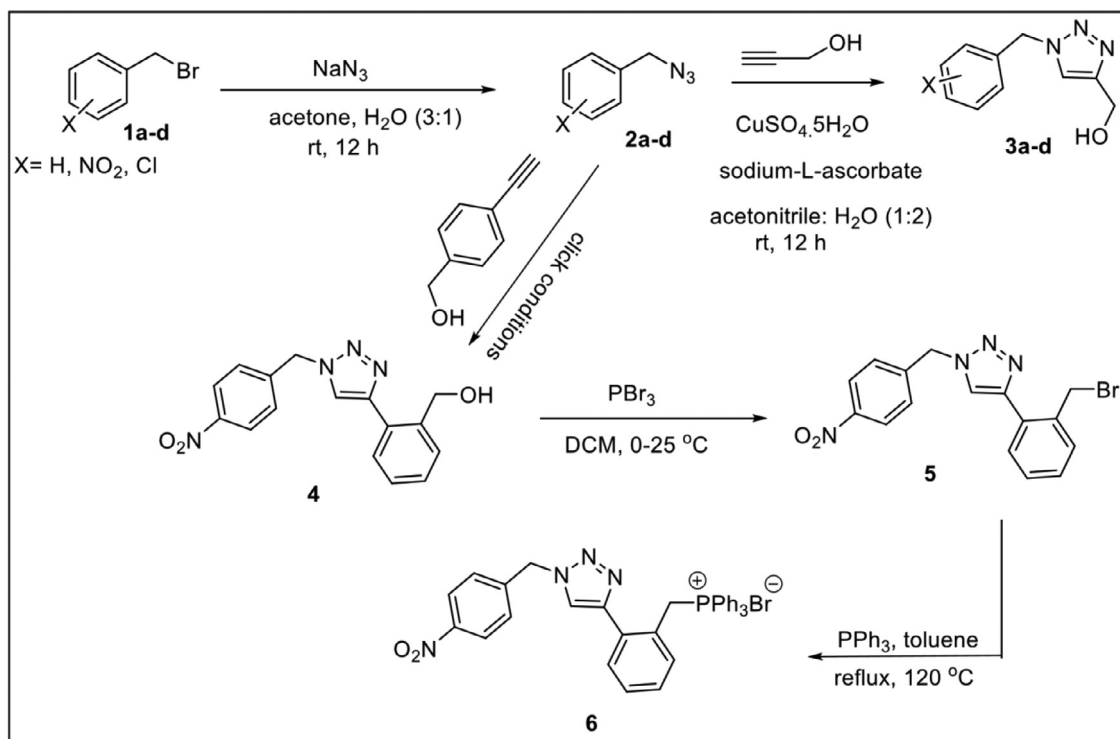
Fig. 3. Scheme for the synthesis of 1,4-disubstituted triazoles and a tethered phosphonium salt (3a-d, 4–6). Click conditions (CuSO$_4$•5H$_2$O, sodium-L-ascorbate, acetonitrile: H$_2$O (1:2), 25 °C, 12 h).

The triazole derivatives and the tethered phosphonium salt were prepared by using commercially available substituted benzyl bromides as limiting reagents. First, the bromo functionality in 1a-d was replaced with the azido group via a simple SN$_2$ reaction using sodium azide in acetone/H$_2$O to afford compounds 2a-d (Fig. 3). The reactive intermediate azides were obtained pure (72–97% yields) as colourless to pale yellow oils and were used immediately for the click reaction. Subsequently compounds 2a-d were subjected to the Cu(I)-catalyzed 1,3-dipolar cycloaddition with the terminal alkyne groups of propargylated alcohol and 2-ethynylbenzyl alcohol afforded the corresponding 1,2,3-triazole-based compounds (73%−98%) as demonstrated in Fig. 1. The 1,2,3-triazole ring acts as a linker connecting the nitro-substituted aryl group and propargyl units. The triazole ring can also introduce an additional binding motif to biological targets through the basic nitrogen atoms. On the other side, the propargyl units attached to the triazole ring provide dual functions: binding of biological targets through the electronegative oxygen atoms and enhancing the solubility of products.

The chemical structures of the 1,4-disubstituted 1,2,3-triazoles (3a-d, 4–6) were fully characterized using different spectroscopic techniques (Figure SM1–SM35). The ^{1}H NMR spectrum of compound 3d, as an example, displayed three signals at δ 8.04, 7.44, and 7.35 ppm, corresponding to the lone proton of the triazole ring and the aromatic multiplet signals respectively. This suggests the presence of connection between the aryl ring with the propargyl part of compound 3d via the heterocyclic 1,2,3-triazole linker. The methylene protons bridging the triazole and the nitroaromatic group are characterised by a singlet signal at 5.59 ppm. The other methylene protons which resonated at 4.52 ppm is characterised by a doublet signal with a corresponding hydroxyl triplet at 5.19 ppm. In the aromatic region, a cluster of multiplets resonating from 7.44 to 7.47 ppm indicated the presence of the nitroaromatic ring. The ^{13}C NMR spectrum of compound 3d showed the cluster of signals from 125 to 150 ppm characteristic of aromatic and heterocyclic carbon signals. Chemical shift signals observed at 52.1 and 55.4 ppm confirmed the presence of methylene Carbon Bridge and the methylene carbon bearing the hydroxyl group respectively. The DEPT-135 NMR confirmed the presence of aliphatic methylene bridge carbon between the triazole and nitroaromatic ring at 52.1 ppm and a propargyl methylene carbon at 55.4 ppm. Signals of quartenary carbons are absent in this spectrum. The ^{13}C-DEPT 135 NMR spectrum of 3d confirmed the presence of three (3) quartenary, three (3) sets of tertiary and six (6) secondary and two (2) secondary. The Electron Spray

Ionization Mass Spectrum (ESIMS) revealed the mass of 224.20 for molecular ion peak [M + H]$^+$ of C$_{10}$H$_{10}$N$_3$O^{35}Cl. The [M + 2] isotopic peak of 226.20 was found for C$_{10}$H$_{15}$N$_3$O^{37}Cl with an established peak ratio of 3:1 [C$_{10}$H$_{10}$N$_3$O^{35}Cl:C$_{10}$H$_{15}$N$_3$O^{37}Cl]. The FTIR spectrum for detecting the functional groups of 3d displayed a weak broad hydroxyl absorption band which slopes from 3284 cm^{-1} into the aliphatic C−H region of 3000 cm^{-1}. The formation of the triazole is confirmed by a medium sharp C−N stretch at ν_{max} of 1128 cm^{-1} corroborated by the presence of medium sharp sp^2−CH stretch at a frequency of 3151cm^{-1}.

For the aromatic (2-ethynylbenzyl alcohol) series, the same click conditions were employed except for the introduction of the terminal alkyne 2-ethynylbenzyl alcohol. The ^{1}H NMR spectrum of compound 4 displayed three signals at δ 8.58, 7.28–8.27 ppm, corresponding to the lone proton of the triazole ring and the aromatic multiplet signals respectively. This points to the connection of the substituted aryl group with the benzene part of compound 4 via the heterocyclic 1,2,3-triazole linker. The methylene protons linking the triazole and the nitroaromatic group are characterised by a singlet signal at 5.88–5.90 ppm. The propargyl methylene protons resonated at 5.75 ppm is characterised by a doublet signal with a corresponding hydroxyl triplet having a chemical shift at 5.00 ppm. In the aromatic region, a cluster of multiplets resonating from 8.27 to 7.28 ppm indicated the presence of the nitroaromatic ring. The ^{13}C NMR spectrum of compound 3d showed the cluster of signals from 124 to 150 ppm characteristic of aromatic and heterocyclic carbon signals. Chemical shift signals observed at 62.0 and 54.0 ppm confirmed the presence of methylene Carbon Bridge and the propargyl methylene carbon on the triazole respectively. The DEPT-135 NMR confirmed the presence of aliphatic methylene bridge carbon between the triazole and nitroaromatic ring at 62.0 ppm and a propargyl methylene carbon at 54.0 ppm. Signals of quartenary carbons are absent in DEPT-135 NMR spectrum. The ^{13}C-DEPT 135 NMR spectrum of compound 4 confirmed the presence of sets of five (5) quartenary, nine (9) tertiary and two (2) secondary.

The Electron Spray ionization Mass Spectrum (ESIMS) revealed an accurate mass of 311.20 for molecular ion peak $[M + H]^+$ $C_{10}H_{10}N_4O_3$. The FTIR spectrum for detecting the functional groups of compound 4 displayed weak broad hydroxyl absorption band which slopes from 3260 cm^{-1} into the aliphatic C–H region of 3000 cm^{-1}. The formation of the triazole is confirmed by a sharp C–N stretch at ν_{max} of 1124 cm^{-1} corroborated by the presence of medium sharp absorbing sp^2 C-H stretch at a frequency of 3083cm^{-1}. A p-nitro substituted 'clicked' product (1,2,3-triazole) was treated with phosphorous tribromide under nitrogen conditions to produce a brominated compound which was our reactive intermediate.

This chemical transformation is evident from the collapse of the triplet hydroxy signal to a singlet peak resonating at 5.80–5.90 ppm in the ^{1}H NMR spectrum of compound 5. The accurate mass provided extra supporting data for the molecular ion peak of $[M + H]^+$ $C_{16}H_{14}N_4O_3{}^{79}Br$ as 373.20 with an $[M + 2]$ peak of 375.20 for $C_{16}H_{14}N_4O_3{}^{81}Br$.

The target compound in the 2-ethynylbenzyl alcohol series is the phosphonium salt (compound 6) and was prepared from compound 5 (bromo compound [aryl halide]) via a nucleophilic substitution bimolecular reaction. The ^{1}H NMR spectrum of compound 6 displayed three signals at δ 8.18, 7.32-7.82 ppm, corresponding to the lone proton of the triazole ring and the aromatic multiplet signals respectively. This confirms the connection of the substituted aryl group with the benzene part of compound 4 via the heterocyclic 1,2,3-triazole linker. The methylene protons linking the triazole and the nitroaromatic group are characterised by a singlet signal at 5.80–5.63 ppm. In the aromatic region, an envelope of multiplets resonating from 7.43 to 7.64 ppm indicated the presence of 15 protons on the phosphonium head. The ^{13}C NMR spectrum of compound 6 showed the cluster of signals between 116 and 150 ppm characteristic of aromatic and heterocyclic carbon signals. Chemical shift signal observed at 52.4 ppm identified the methylene carbon bridge. The signals at 27.3 and 27.1 ppm represented a doublet signal for the methylene carbon associated with the phosphonium head and the phosphorous (ipso carbon) respectively. The High Resolution Electron Spray ionization Mass.

Spectrum (MS) of compound 6 revealed the accurate mass of 555.40 for molecular ion peak $C_{34}H_{28}N_4O_2P^+$. The FTIR spectrum for detecting the functional groups of compound 6 displayed weak broad hydroxyl absorption band which slopes from 3284 cm^{-1} into the aliphatic C–H region of 3000 cm^{-1}. The formation of the triazole is confirmed by a sharp C–N stretch at ν_{max} of 1154 cm^{-1} corroborated by the presence of medium sharp absorbing sp^2 C-H stretch at a frequency of 3151cm^{-1}.

Antimalarial assay. The biological assay involved the evaluation of the antimalarial activity of the seven (7) compounds against the trophozoite ring stage of chloroquine resistant Plasmodium falciparum DD2 lab strain using chloroquine and artesunate as reference drugs. Quinine and chloroquine have maintained their antimalarial efficacy for several years before the inception of artemisinin (ART) and artemisinin-based combination therapy (ACT). The widely recommended therapy to control malaria is currently under threat from resistance strains of Plasmodium falciparum. This reinforces the quest for new lead compounds with high efficacy and low toxicity. Most antimalarials such as chloroquine, quinine and artemisinins act on the erythrocytic stages of the parasite during the process of infection hence terminates the attack of malaria and halting the threat of resistance which makes it a conventional method of in vitro antimalarial assay aside its simplicity and cost-effectiveness [37].

The SYBR Green-I fluorescence assay is a conventional method in interpretation of the Plasmodium inhibition data. In this study seven (7) compounds were analysed for antimalarial activity and the results showed good activity for three (3) of the compounds against chloroquine resistant DD2 lab strain (0.62–0.65 ug/ml) as shown in Table 1.

From Table 1, the antimalarial activity of triazoles related to the position of nitro groups on the aromatic ring.

Artesunate and Chloroquine = positive control [a] IC$_{50}$ and [b] CC$_{50}$ values represent duplicate determinations (two determinations from three different experiments).

Concerning the aromatic ring, the most successful was the nitro derivatives 3a, 3b and 3c. They had similar potency an IC$_{50}$ of 0.62–0.65 ug/ml. One striking observation which could account for the high IC$_{50}$ values of the remaining four compounds is lipophilicity which can be quantified by their clogP. The presence of chlorine in compound 3d provided an increased clogP and could have decreased the in vitro antimalarial activity because of low plasma solubility under the conditions of the in-vitro assay. For compounds 4, 5 and 6, there was no antimalarial activity recorded and was represented as ambiguous from the

Table 1

In-vitro antimalarial activity (IC$_{50}$), cytotoxicity profile (CC$_{50}$) and selectivity index (SI) of the compounds.

Compounds	IC$_{50\pm SEM\ (\mu g/ml)}$ [a]	CC$_{50\pm SEM\ (\mu g/mL)}$ [b]	SI [c]
3a	0.62 ± 0.036	> 100	>161
3b	0.64 ± 0.092	87.380 ± 0.91	136
3c	0.65 ± 0.071	75.496 ± 0.94	116
3d	22.11 ± 3.708	88.637 ± 0.65	4
4	> 100	33.320 ± 1.21	0.33
5	> 100	>100	>1
6	> 100	>100	>1
Artesunate	$2.3 \times 10^{-3} \pm 1.9 \times 10^{-5}$	>100	>1000
Chloroquine	$7.3 \times 10^{-2} \pm 0.548$	>100	>1000

Key: [a] IC$_{50}$= 50% inhibitory concentration on Plasmodium falciparum chloroquine resistant strain (Dd2); lowest IC$_{50}$: highest antiplasmodial activity [b] CC$_{50}$ =50% cytotoxic concentration on human erythrocytes. SI [c] =Selective index (CC$_{50}$/IC$_{50}$); SI >1 means low cytotoxicity.

Table 2

In silico physicochemical and pharmacokinetic parameters of synthesized compounds.

Compound	Molecular weight	Physicochemical parameters							
		cLogP	H-bond Donor	H-bond Acceptor	TPSA (140 Å^2)	Rotatable Bonds	Number of atoms	Violation	% ABS
3a	234.22	0.73	1	6	94.08	4		0	76.56
3b	234.22	0.73	1	6	94.08	4		0	91.43
3c	234.22	0.73	1	6	94.08	4		0	76.56
3d	223.66	1.47	1	4	50.94	3		0	76.56
4	310.31	2.39	1	6	94.08	5		0	76.56
5	373.21	3.80	0	5	73.85	5		0	83.52
6	635.50	3.40	0	5	–	9		1	–

cLog P: Calculated lipophilicity, H-bond Donor: Number of hydrogen bond donors, H-bond Acceptor: Number of hydrogen bond acceptors, TPSA: Polar surface area (Å^2), Violation: Number of violations from Lipinski's rule of five,%ABS: Absorption percentage .

GraphPad Prism version 7 analysis suggesting that the IC$_{50s}$ were far greater than 100 μg/ml for each compound (highest concentration used in the assay). Hence the presence of an extra aromatic group at position 4 on the triazole in compound 4, the propargyl bromo in compound 5 and envelope of hydrophobic aromatic groups in the phosphonium salt (compound 6) rendered them inactive against the resistant Plasmodium falciparum (DD2) lab strain. The clogP values of compounds 3d, 4, 5 and 6 were 0.913, 1.741, 3.561 and 8.538 respectively demonstrating an increased lipophilicity compared to the most active triazoles (3a-c). Further, to investigate cytotoxic effects of all the triazole hybrids, results indicate very minimal cytotoxicity of 3a-d with selectivity indices greater than 1 (Table 1). Considering the suitability of these compounds as suitable candidates for oral use, the Lipinski's rule of five was used as a benchmark. Lipinski's rule of five is based on the following criteria: the compound must have; less than 5 hydrogen bond donors, less than 10 hydrogen bond acceptors, less than 500 Daltons molecular weight and octanol: water partition co-efficient (logP or clogP) less than 5. It can be observed from Table 2 that all the 3a-d, 4 and 5, the most active triazoles passed criteria.

1–4 except compound 6 (phosphonium salt) which has a molecular weight of 555.4100 and clog P of 8.538. This means that going forward, there should be molecular fragmentation of compound 6 so as to meet all the Lipinski's rules.

On the other hand, the selectivity index (SI) is defined as the relative efficacy of a candidate compound in inhibiting cell multiplication as compared to inducing cell death. Hence, it is preferable to have higher selectivity index that means high activity with least cellular damage [38]. The comparison of the selectivity indices obtained for compounds 3a-c and demonstrates good therapeutic effect since the SI values are greater than 1 (Table 1). The triazole 3a has comparatively higher CC$_{50}$ values (> 100 μg/mL) and good selectivity index (161) that demonstrates optimal selective antimalarial activity. Out of the most active triazoles, compound 3d bearing the chloro group exhibited the highest in vitro cytotoxicity. The most toxic of the compounds were 4, 5 and 6 whose IC$_{50s}$ values suggested from the GraphPad Prism software to be far greater than the highest concentration used in the assay. The percentage viability of the erythrocytes in the MTT assay showed that compound 5 had less structural damage however since its IC$_{50}$ could not be determined, the SI was less than 2 rendering it cytotoxic. Compounds 4 and 6 also did not inhibit the ring stage of the parasite making them have ambiguous readings (> 100 μg/mL for each compound) hence worth further investigation to know about factors that might contributed to their antiplasmodial inactivity. However, compounds 3a-c have proved to be effective with low cytotoxicity to human erythrocytes hence worth considering as lead compounds.

Some isolated compounds: genistin, malonylgenistin and genistein showed the lowest antiplasmodial activity (7.867, >10 and 7.736 μg/mL, respectively) and the most cytotoxic (IC$_{50}$ of 168.6, 181.9 and 116.1 μg/mL, respectively) compared to other isolates from the roots of E. montanum [38]. This gives them a SI of 24.9, nd and 15.0 respectively for the three compounds which were all >1 making them most cytotoxic compared to the other compounds isolated from the plant's roots. All the synthesised compounds except 4 had SI >1 making them less cytotoxic than the plant's isolates.

Table 3
Predicted toxicity profile of synthesized compounds.

Compound	hERG Inhibition	Carcinogenicity	Mutagenicity	Hepatotoxicity	Acute Oral toxicity
3a	–	–	+	+	III
3b	–	–	–	+	III
3c	–	–	+	+	III
3d	–	–	–	+	III
4	–	–	+	+	III
5	–	–	+	+	III
6	–	–	+	+	III

In silico assessment of the pharmacokinetic and toxicity profiles of the synthesized compounds were carried out to predict their drug-like properties. This is of particular importance because 40% of failed clinical trials have been attributed to poor absorption, distribution, metabolism and excretion (ADME) properties of the drug candidates [39]. The compounds except for the phosphonium salt exhibited good tendencies for oral bioavail-abilities by recording Topological polar surface area (TPSA) values ranging from 50.94 to 94.08 Å^2. The compounds having TPSA values $\leq$ 140 Å^2 indicate that they possess good cell permeability and transport properties and therefore have oral bioavailability. It was therefore not surprising they were predicted to have good percentage (%) absorption from of 76% to 91%.

Pharmacokinetic effects and toxicity of synthesised compounds 3a-d, 4–6

All the compounds complied with Lipinski's rule of oral drug, except for the phosphonium salt which violated one having a molecular weight < 500. Again, the compounds, apart from the phosphonium salt, recorded TPSA values < 140 Å^2 (50.94 – 94.08 Å^2) and percentage absorption of 76 – 91% indicating they have good permeability and oral bioavailability (Table 2). The TPSA value of the phosphonium salt could not be predicted by the software which can be attributed to its rather large and unusual size. All the compounds exhibited hepatotoxic and mutagenic toxicity tendencies apart from 3b and 3d which displayed potential for only liver toxicities. They were classified as category III acute oral toxins (Table 3).

Again, most of the compounds complied fully with Lipinski's rule-of-5 for orally active drugs (Abdullahi & Elijah, 2020; Paramashivam et al., 2015) [39] by recording molecular weight $\leq$ 500, logP (lipophilicity) $\leq$ 5, number of hydrogen bond donors $\leq$ 5 and number of hydrogen bond acceptors $\leq$10 with the exception of the phosphonium salt which had one violation, molecular weight $\leq$ 500. With this, it can be said that the compounds have the potential to be developed into drug candidates as none showed no more than one violation of the rule. The compounds were predicted to be slightly toxic exhibiting mutagenic and hepatotoxic potentials which need to be addressed during the optimization stages of the drug development. They were thus placed in category III of acute oral toxins possessing LD$_{50}$ from 500 to 5000 mg/kg. Further optimization could therefore focus on improving their toxicity profiles.

Molecular docking

Molecular docking was used to explore the binding poses of compound 3a-3d in the protein active sites of each of the four (4) proteins investigated. The docking protocol used for each protein was validated by superimposition of re-docked poses of co-crystallized ligands with crystal conformations extracted from the PDB. Overall, ligand binding potentials varied between-7.5 and-5.6 kcal/mol (Table SM1). For PfHDP, the binding constants for the 4 ligands ranged from-6.90 kcal/mol to-7.40 kcal/mol. The binding constants obtained for Plms IV (−6.20 to-6.60 kcal/mol), Plms II (−5.80 to-6.00 kcal/mol) and PfFP2 (−5.60 to-6.00 kcal/mol) were poorer in comparison to those of PfHDP. In terms of binding affinity, the order of potential inhibitory action of the triazoles was in the order of PfHDP > Plms IV > Plms II > PfFP2. Thus, the ligands had high affinities for both PfHDP and PlmsIV, compared to moderate affinity recorded for PfFP2 and Plms II. The binding affinities of compounds 3a-3d, ligand efficiencies, together with their non-bonding interactions, correlate well with the in vitro activity observed. In particular, compound 3b produced a high affinity for all protein targets. Molecular recognition is driven by very strong hydrogen bonding interactions between the ligand and catalytic pocket residues. For instance, hydrogen bonding of nitro-groups with Arg4 was twice as short in 3a as in 3b, hence the-0.1 kcal/mol difference in binding potential. Additionally, observed hydrophobic and Van der Waal's interactions with inhibitor pocket and interface residues could be essential for inhibition of the Dsq protein complex. Overall, high ligand affinities were obtained for PfHDP and Plms IV (Fig. SM43). Hence, compounds 3a-3d could potentially obstruct the kinetics of hemoglobin digestion and heme polymerization (Figure SM40-SM46). Recently, a series of artemisin-peptidyl vinyl phosphonate hybrid molecules have been shown to possess superior efficacy than artemisinin alone against chloroquine and multigrug resistant P. falciparum. The molecules were shown to inhibit falcipain 2 activity as well as PfHDP activity by blocking hemozoin formation [40]). This highlights the importance of flexible molecules in interacting with the heme binding domain of PfHDP in particular. The results obtained from the molecular docking study suggest that interaction of the triazoles with proteases and enzymes that make up the P. falciparum degradosequesterome may contribute to the inhibition of P. falciparum, as observed in the in vitro data.

Conclusion

Six (6) novel 'clicked' compounds and a 'clicked'-tethered phosphonium salt have been successfully synthesised and characterised using their melting point, ^{1}H, ^{13}C, DEPT-135 NMR, IR and MS data. They have been explored for their potential as antimicrobial agents against pathogenic strains. The significantly active compounds against the trophozoite (ring) stage of chloroquine resistant Plasmodium falciparum DD2 lab strain included (1-(4-nitrobenzyl)−1H-1,2,3-triazole-4-yl)methanol (3a), (1-(3-nitrobenzyl)−1H-1, 2, 3-triazole4-yl) methanol (3b), (1-(2-nitrobenzyl)−1H-1,2,3-triazole-4-yl)methanol (3c) and (1-(4-chlorobenzyl)1H-1,2,3-triazole-4-yl)methanol (3d).

These compounds did not have any cytotoxic effect on human erythrocytic cells. On the other hand, compound 4 was the most cytotoxic to human erythrocytic cells since it had the lowest selectivity index (SI) of 0.33 whilst 3a had the highest SI of 161, establishing the lowest cytotoxicity. The antimalarial importance of the 1,2,3-triazole in medicinal compounds has been confirmed and the current study has provided structure-activity relationship information for future lead optimization. To the best of our knowledge, this is the first ever report on the antimalarial and antimicrobial potential of these compounds. From the ADME predictions, it can be said that the compounds can be developed into oral drug candidates as none showed more than one violation of Lipinski's rule despite exhibiting some mutagenic and hepatotoxic potential. Moreover, the results of molecular docking studies suggest that interaction of the triazoles with the proteins of the P. falciparum degradosequesterome may play a role in their inhibitory action. Compounds 3a-d could therefore act as structural scaffolds for the development of novel antimalarials.

Supporting information attached.

Author's contributions

A.B., J.N.A, C.D.K.A designed the research study, F.K.K., C.D.K.A., F.K.Z., B.K.H., E.O., C.A. and M.T. provided the resources, F.K.K., C.D.K.A P.P. and B.K.H. conducted the synthesis, characterization and in-silico studies, F.K.Z. and E.O performed the antimalarial study, L.S.B. and E.N.G. performed the molecular docking studies, C.D.K.A, F.K.K, A.B., J.N.A, L.S.B. and E.N.G. prepared the draft manuscript, C.D.K.A., A.B., C.A., L.S.B., E.N.G. and B.K.H conducted writing-review and edit. All authors have read and approved the final manuscript.

Data availability

All data regarding this research can be found at the Faculty of Pharmacy and Pharmaceutical Sciences, Kwame Nkrumah University of Science and Technology.

Funding

Declaration of competing interest

The authors report no conflicts of interest. The authors alone are responsible for the content and writing of the paper.

Acknowledgments

References

[1] R.J. Fair, Y. Tor, 'Antibiotics and bacterial resistance in the 21st Century, Perspect Medicin Chem 6 (2014) 25–64, doi:10.4137/PMC.S14459.
[2] Y. Furuse, Analysis of research intensity on infectious disease by disease burden reveals which infectious diseases are neglected by researchers, PNAS J. 116 (2) (2019) 478–483 https://doi.org/10.1073/pnas.1814484116.
[3] A.R. Coates, G. Halls, Y. Hu, "Novel classes of antibiotics or more of the same? Br. J. Pharmacol. 163 (1) (2011) 184–194 https://doi.org/10.1111/j.1476-5381.2011.01250.x.
[4] S. Santajit, N. Indrawattana, Mechanisms of antimicrobial resistance, in: ESKAPE Pathogens, BioMed Research International, 2016, pp. 1–8. 2016https://doi.org/10.1155/2016/2475067.
[5] L.C. Steinhardt, A.J. Magill, P.M. Arguin, 'Review: malaria chemoprophylaxis for travellers to Latin America, Am. J. Trop. Med. Hyg. 85 (6) (2011) 1015–1024, doi:10.4269/ajtmh.2011.11-0464.
[6] S. Haque, D.A. Nawrot, S. Alakurtti,, L. Ghemtio, J. Yli-kauhaluoma, 'Screening and Characterisation of Antimicrobial Properties of Semisynthetic Betulin Derivatives, PLoS ONE 9 (7) (2014) e102696 2014, doi:10.1371/journal.pone.0102696.
[7] S. Krishna, L. Bustamante, R.K. Haynes, H.M. Staines, 'Artemisinins: their growing importance in medicine, Trends Pharmacol. Sci. 29 (10) (2008) 520–527, doi:10.1016/j.tips.2008.07.004.
[8] A.D. Forkuo, C. Ansah, K.M. Boadu, J.N. Boampong, E.O. Ameyaw, B.A. Gyan, et al., 'Synergistic anti – malarial action of cryptolepine and artemisinins, Malar. J. 15 (89) (2016), doi:10.1186/s12936-016-1137-5.

[9] P. Chitnumsub, J. Aritsara, T. Yuwadee, N. Krittikar, L. Benjamas, P. Sinothai, et al., The structure of plasmodium falciparum Hydroxymethyldihydropterin Pyrophosphokinase-dihydropteroate synthase reveals the basis of sulfa resistance, FEBS J. 287 (15) (2020) 3273–3297, doi:10.1111/febs.15196.

[10] Philip J. Rosenthal, Chapter 437 - Falcipains, in: Neil D. Rawlings, Guy Salvesen (Eds.), Handbook of Proteolytic Enzymes (Third Edition), edited by, Academic Press, 2013, pp. 1907–1912, doi:10.1016/B978-0-12-382219-2.00436-1.

[11] M. Chugh, V. Sundararaman, S. Kumar, V.S. Reddy, A.W. Siddiqui, K.D. Stuart, et al., 'Protein complex directs hemoglobin-to-hemozoin formation in Plasmodium falciparum, in: Proceedings of the National Academy of Sciences of the United States of America, 110, 2013, pp. 5392–5397, doi:10.1073/pnas.1218412110.

[12] K.A. De Villiers, Egan Recent advances in the discovery of haem-targeting drugs for malaria and schistosomiasis, Molecules 14 (8) (2009) 2868–2887, doi:10.3390/molecules14082868.

[13] B.J. Dame, C.A. Yowell, L. Omara-Opyene, J.M. Carlton, R.A. Cooper, T. Li, Plasmepsin 4, the food vacuole aspartic proteinase found in all plasmodium Spp. Infecting Man, Mol. Biochem. Parasitol. 130 (1) (2003) 1–12, doi:10.1016/S0166-6851(03)00137-3.

[14] N. Dan, S. Bhakat, New paradigm of an Old Target: an update on structural biology and current progress in drug design towards Plasmepsin II, Eur. J. Med. Chem. 95 (May) (2015) 324–348, doi:10.1016/j.ejmech.2015.03.049.

[15] Peng. Liu, Plasmepsin: Function, Characterization and Targeted Antimalarial Drug Development, Natural Remedies in the Fight Against Parasites. IntechOpen, 2017, doi:10.5772/66716.

[16] D. Jani, N. Rana, B. Wandy, A. Ross, C. Slebodnick, J. Andersen, et al., HDP—A novel heme detoxification protein from the malaria parasite, PLoS Pathog. 4 (4) (2008) e1000053, doi:10.1371/journal.ppat.1000053.

[17] P. Gupta, S. Mehrota, A. Sharma, M. Chugh, J. Pandey, A. Kaushik, et al., Exploring heme and hemoglobin binding regions of plasmodium heme detoxification protein for new antimalarial discovery, J. Med. Chem. 60 (2) (2017) 8298–8308, doi:10.1021/acs.jmedchem.7b00089.

[18] C. Singh, H. Malik, S.K. Puri, Synthesis and antimalarial activity of a new series, ACS publ. 12 (15) (2004) 1177–1182, doi:10.1016/j.bmc.2003.11.021.

[19] B. Kwansa-Bentum, K. Agyeman, J. Larbi-Akor, C. Anyigba, R. Appiah-Opong, In Vitro Assessment of Antiplasmodial Activity and Cytotoxicity of Polyalthia Longifolia Leaf Extracts on Plasmodium Falciparum Strain NF54", Malaria Research and Treatment, 2019, doi:10.1155/2019/6976298.

[20] S. Behrouz, Highly efficient three-component synthesis of 5-substituted-1 H -tetrazoles from aldehydes, hydroxylamine, and tetrabutylammonium azide using doped nano-sized copper (I) oxide on melamine – formaldehyde resin, J. Saudi Chem. Soc. 22 (18) (2016), doi:10.1016/j.jscs.2016.08.003.

[21] H.C. Kolb, M.G. Finn, Sharpless click chemistry: diverse chemical function from a few good reactions, Angewandte Chemie 40 (11) (2001) 2004–2021 PMID: 11433435.

[22] C.E. Diesendruck, L. Zhu, J.S. Moore, "Alkyne mechanochemistry: putative activation by transoidal bending, Chem. Commun. 50 (2014) 13235–13238, doi:10.1039/C4CC03514C.

[23] Y.H. Zhang, Z.X. Gao, C.L. Zhong, H.B. Zhou, L. Chen, W.M. Wu, et al., An inexpensive fluorescent labeling protocol for bioactive natural products utilizing Cu(I)-Catalyzed Huisgen reaction, Tetrahedron 63 (2007) 6813–6821.

[24] S. Rohilla, S. Patel, N. Jain, Copper acetate catalyzed regioselective synthesis of substituted 1,2,3-Triazoles: a Versatile Azide – Alkene cycloaddition-oxidation approach", Eur. J. Org. Chem. 4 (2016) 847–854, doi:10.1002/ejoc.201501301.

[25] D. Pasini, The click reaction as an efficient tool for the construction of macrocyclic structures, Molecules 8 (2013) 9512–9530, doi:10.3390/molecules18089512.

[26] M. Aufort, J. Herscovici, P. Bouhours, N. Moreau, C. Girard, 'Synthesis and antibiotic activity of a small molecules library of 1, 2, 3-triazole derivatives,", Bioorganic Med. Chem. Lett. 18 (2008) 1195–1198, doi:10.1016/j.bmcl.2007.11.111.

[27] A. Haslop, A. Gee, C. Plisson, N. Long, 'Fully automated radiosynthesis of [1-(2[18F]fluoroethyl),1H[1, 2,3]triazole 4-ethylene] triphenylphosphonium bromide as a potential positron emission tomography tracer for imaging apoptosis, J. Labelled Compound Radiopharmaceutic. 56 (6) (2013) 313–316, doi:10.1002/jlcr.3024.

[28] P.A. Ravindra, S. Karpagam, Synthesis and biological activity of Azine heterocycle functionalized quaternary phosphonium salts, IOP Conference Series: Materials Science and Engineering, 263, 2017, doi:10.1088/1757-899X/263/2/022017.

[29] A. Amati, G. Dosualdo, L. Zhao, A. Bravo, F. Fontana, F. Minisci, et al., 'Catalytic processes of oxidation by hydrogen peroxide in the presence of Br$_2$ or HBr mechanism and synthetic applications, Organ. Process Res. Dev. 2 (1998) 261–269.

[30] X.M. Chu, C. Wang, W.L. Wang, L.L. Liang, W. Liu, K.K. Gong, et al., 'Triazole derivatives and their antiplasmodial and antimalarial activities, Eur. J. Med. Chem. 166 (2019) 206–223, doi:10.1016/j.ejmech.2019.01.047.

[31] L. Cui, Z. Wang, J. Miao, M. Miao, R. Chandra, H. Jiang, et al., 'Mechanisms of in vitro resistance to dihydroartemisinin in Plasmodium falciparum, Mol. Microbiol. 86 (1) (2012) 111–128, doi:10.1111/j.1365-2958.2012.08180.x.

[32] Y. Liu, K. Cui, W. Lu, W. Luo, J. Wang, J. Huang, et al., Synthesis and antimalarial Activity of Novel Dihydro-Artemisinin derivatives, Molecules 16 (6) (2011) 4527–4538, doi:10.3390/molecules16064527.

[33] S.K. Paramashivam, K. Elayaperumal, N. Kalaivani, R. Boopala, M. Balasubramanian, K.N. Dhiraviam, ' In silico pharmacokinetic and molecular docking studies of small molecules derived from Indigofera aspalathoides Vahl" targeting receptor tyrosine kinases, Bioinformation 11 (2015) 73–84, doi:10.6026/97320630011073.

[34] J.M. Machin, A.L. Kantsadi, I. Vakonakis, 'the complex of Plasmodium falciparum falcipain-2 protease with an (E)-chalcone-based inhibitor highlights a novel, small, molecule-binding site, Malaria J. BioMed Central 18 (2019) 1–9, doi:10.1186/s12936-019-3043-0.

[35] L.S. Borquaye, E.N. Gasu, G.B. Ampomah, L.K. Kyei, M.A. Amarh, C.N. Mensah, et al., in: "Alkaloids from Cryptolepis sanguinolenta As Potential Inhibitors of SARS-CoV-2 Viral Proteins : An In Silico Study,, 5324560, BioMed Research International, Research, 2020, pp. 1–14, doi:10.1155/2020/5324560.

[36] D.F. Veber, S.R. Johnson, H.Y. Cheng, B.R. Smith, K.W. Ward, K.D. Kopple, 'Molecular properties that influence the oral bioavailability of drug candidates, J. Med. Chem. 45 (12) (2002) 2615–2623 PMID: 12036371.

[37] X. Xin, Y. Vugmeyster, 'Challenges and opportunities in absorption, distribution, metabolism, and excretion studies of therapeutic biologics, AAPS J. 14 (2012) 781–791, doi:10.1208/s12248-012-9388-8.

[38] J. Tomani,. C.D. Bonnet, O. Nyirimigabo, A. Deschamps, W. Tchinda, A.T. Jansen, et al.,. "In vitro antiplasmodial and cytotoxic activities of compounds from the roots of eriosema montanum baker f.(fabaceae)". Molecules, vol. 26, no. 9, 1–9. 2021https://doi.org/10.3390/molecules26092795.

[39] M. Abdullahi, S. Elijah, In – silico molecular docking and ADME /Pharmacokinetic prediction studies of some novel carboxamide derivatives as Anti – tubercular Agents, Chem. Africa (2020) 0123456789, doi:10.1007/s42250-020-00162-3.

[40] E.K. Aratikatla, M.D. Kalamuddin, R.C. Kalpeshkumar, D. Gaurav, A. Mohd, S. Srividhya, et al., Combating multi-drug resistant malaria parasite by inhibiting falcipain-2 and heme-polymerization: artemisinin-Peptidyl Vinyl phosphonate hybrid molecules as new antimalarials, Eur. J. Med. Chem. 220 (2021) 113454.